MULTIPLE SNAPSHOT COMPRESSIVE BEAMFORMING

Peter Gerstoft[1]*, Angeliki Xenaki*[2]*, Christoph F. Mecklenbräuker*[3]*, and Erich Zöchmann*[3]

[1] University of California, San Diego, CA 92093-0238, USA,
gerstoft@ucsd.edu
[2] Department of Electrical Engineering, Technical University of Denmark, 2800 Denmark
[3] Christian Doppler Lab, Inst. of Telecommunications, TU Wien, 1040 Vienna, Austria,

ABSTRACT

For sound fields observed on an array, compressive sensing (CS) reconstructs the multiple source signals at unknown directions-of-arrival (DOAs) using a sparsity constraint. The DOA estimation is posed as an underdetermined problem expressing the field at each sensor as a phase-lagged superposition of source amplitudes at all hypothetical DOAs. CS is applicable even for a single observation snapshot achieving a higher resolution than conventional beamforming. For multiple snapshots, CS outperforms conventional high-resolution methods, even with coherent arrivals and at low signal-to-noise ratio.

1. INTRODUCTION

Direction-of-arrival (DOA) estimation refers to the localization of several sources from noisy measurements of the wavefield with an array of sensors. Thus, DOA estimation is expressible as a linear underdetermined problem with a sparsity constraint enforced on its solution. Compressive sensing (CS) asserts that this is solved efficiently with a convex optimization procedure which promotes sparse solutions. In DOA estimation, CS achieves high-resolution acoustic imaging [1, 2, 3], outperforming traditional methods [4]. Unlike the subspace DOA estimation methods which also offer super-resolution, DOA estimation with CS is reliable even with a single snapshot [5, 6, 7].

For multiple snapshots, CS has benefits over other high-resolution beamformers [1, 2, 8]:
1) It does not require the arrivals to be incoherent.
2) It can be formulated with any number of snapshots, in contrast to eigenvalue based processors, as the Minimum Variance Distortion-free Response (MVDR) beamformer.
3) Its flexibility in the problem formulation enables extensions to sequential processing, and online algorithms.
We show here that CS obtains higher resolution than MVDR, even in scenarios which favor classical high-resolution methods. A more in-depth analysis and longer version of this paper can be found in Ref. [8].

2. MULTIPLE-SNAPSHOT DOA ESTIMATION

Even though for moving sources it benefits to solve one optimization problem for each snapshot sequentially, for stationary scenarios, it is expected that an improved estimate is achievable by aggregating the sensor data statistics over multiple snapshots in time. Multiple snapshots are referred to as multiple measurement vectors and the recovery might have better performance than single measurement vectors [9, 10]. Potentially the recovery can be made more robust by using a likelihood function with colored noise (full covariance matrix) or based on the Huber norm [11].

Assuming aggregation over L snapshots, the sensor data model becomes

$$\mathbf{Y} = \mathbf{A}\mathbf{X} + \mathbf{N}\,, \tag{1}$$

where, $\mathbf{Y} = [\mathbf{y}(1), \cdots, \mathbf{y}(L)]$ and $\mathbf{N} = [\mathbf{n}(1), \cdots, \mathbf{n}(L)]$ are $M \times L$ matrices with the measurement and noise vectors per snapshot as columns, respectively, and $\mathbf{X}$ is the $N \times L$ signal with the complex source amplitudes at the N DOAs per snapshot as columns. For stationary sources the matrix $\mathbf{X} = [\mathbf{x}(1), \cdots, \mathbf{x}(L)]$ exhibits row sparsity, i.e., it has a constant sparsity profile for every column, since the few existing sources are associated with the same DOA for all snapshots.

As the sources are stationary it makes sense to sum the source energy across all snapshots, giving the row norm $\mathbf{x}^{\ell_2}$

$$\mathbf{x}^{\ell_2} = \left(\sum_{l=1}^{L} |\mathbf{X}_{\cdot l}|^2 \right)^{1/2} . \tag{2}$$

This quantity is sparse and in analogy with the single snapshot case we impose a Laplacian-like prior for the magnitude

$$p(\mathbf{X}) = p(\mathbf{x}^{\ell_2}) \propto \exp(-\|\mathbf{x}^{\ell_2}\|_1/\nu). \tag{3}$$

We assume the phase is uniformly iid distributed on $[0, 2\pi)$.

We assume an iid complex Gaussian distribution for the data likelihood

$$p(\mathbf{Y}|\mathbf{X}) \propto \exp(-\|\mathbf{Y} - \mathbf{A}\mathbf{X}\|_{\mathcal{F}}^2/\sigma^2). \tag{4}$$

Using Bayes theorem, the MAP solution is then

$$\begin{aligned}\widehat{\mathbf{X}} &= \arg\max p(\mathbf{Y}|\mathbf{X})p(\mathbf{X}) \\ &= \underset{\mathbf{X}\in\mathbb{C}^{N\times L}}{\arg\min} \|\mathbf{Y}-\mathbf{A}\mathbf{X}\|_{\mathcal{F}}^2 + \mu\|\mathbf{x}^{\ell_2}\|_1.\end{aligned} \tag{5}$$

In this formulation we search for a sparse solution via the ℓ_1 constraint. The source amplitude can, however, vary across snapshots. This is in contrast to covariance-matrix based beamforming that just inverts for the average source power. The processing performance can be improved by doing an eigenvalue decomposition of $\mathbf{X}$ and retaining just the largest eigenvalues [1, 2]. The smaller eigenvalues contain mostly noise so this improves processing. However, this eigenvalue decomposition is not done here as this has features similar to forming a sample covariance matrix.

Once the active steering vectors have been recovered, the unbiased source amplitudes are estimated for each snapshot, similar to the single snapshot case [6]

$$\widehat{\mathbf{X}}_{\text{CS}} = \mathbf{A}_\alpha^+\mathbf{Y}, \tag{6}$$

Where $\mathbf{A}_\alpha$ is the active columns corresponding to the sparse solution (5) and $^+$ is the Moore-Penrose inverse. If desired, an average power estimate $\mathbf{x}_{\text{CS}}^{\ell_2}$ can be obtained from the ℓ_2-norm of the rows of $\widehat{\mathbf{X}}_{\text{CS}}$, with the ith element squared of $\mathbf{x}_{\text{CS}}^{\ell_2}$ being the source power estimate at θ_i.

2.1. DOA estimation error evaluation

If the source DOAs are well separated with not too different magnitudes, the DOA estimation for multiple sources using CBF and CS turns out to behave similarly. They differ, however, in their behavior whenever two sources are closely spaced. The same applies for MVDR under the additional assumptions of incoherent arrivals and sufficient number of snapshots, $L \geq M$. The details are of course scenario dependent.

For the purpose of a quantitative performance evaluation with synthetic data, the estimated, $\widehat{\theta}_k$, and the true, θ_k^{true}, DOAs are paired with each other such that the root mean squared DOA error is minimized in each single realization. After this pairing, the ensemble root mean squared error is computed over the K active sources,

$$\text{RMSE} = \sqrt{\text{E}\left[\frac{1}{K}\sum_{k=1}^{K}(\widehat{\theta}_k - \theta_k^{\text{true}})^2\right]}. \tag{7}$$

CBF suffers from low-resolution and the effect of sidelobes for both single and multiple data snapshots, thus the simple peak search used here is too simple. These problems are reduced in MVDR for multiple snapshots and they do not arise with CS,

In the following simulation study, we consider an array with $M = 20$ elements and intersensor spacing $d = \lambda/2$. The DOAs for plane wave arrivals are assumed to be on a fine angular grid $[-90°{:}0.5°{:}90°]$. The CS solution is found using the least absolute shrinkage and selection operator (LASSO) [12] which has been extended to multiple measurement vectors (here multiple snapshots) [8, 13].

Estimating the source DOAs based on $L = 50$ snapshots gives the results in Fig. 1. At $\text{SNR} = 0\,\text{dB}$ the diagrams in Fig. 1a show that CS localizes the sources well, in contrast to the CBF and MVDR that is also indicated in the histograms in Fig. 1b. The RMSE in Fig. 1c, shows that CBF does not give the required resolution even for high SNR. MVDR performs well for $\text{SNR} > 10\,\text{dB}$, whereas CS performs well for SNRs down to $2.5\,\text{dB}$.

The weak broadside sources are moved closer with DOAs defined as $[-2,\ 1,\ 75]°$. Fig. 2 gives about the same DOA estimates for CBF, as it is already at its maximum performance even for high array SNR, confirming its low resolution. MVDR fails for $\text{SNR} < 20\,\text{dB}$, which is $10\,\text{dB}$ higher than the corresponding value in Fig. 1c (MUSIC fails also at a level $10\,\text{dB}$ higher). Contrarily, CS fails only for $\text{SNR} < 5\,\text{dB}$ which is $2.5\,\text{dB}$ higher (Figs. 1c and 2c). Note how MVDR completely misses the weak source at $-2°$ in Figs. 2c, but CS localize it with a larger spread. Thus, as the weak source moves closer to the strong source, CS degrades slower than MVDR in terms of RMSE. This is a good indication of its high-resolution capabilities.

Figure 3 shows the estimated power at the one realization in Fig. 1a of $L = 50$ snapshots inverted simultaneously. We emphasize the scale of the problem. Equation (1) has $20 \cdot 50 = 1000$ equations to determine $361 \cdot 50 = 18050$ complex-valued variables at 361 azimuths and 50 snapshots observed on 20 sensors. The sparsity constraint is crucial here.

3. EXPERIMENTAL RESULTS

The high-resolution performance of CS both in single- and multiple-snapshot cases is validated with experimental data in a complex multi-path shallow-water environment and it is compared with conventional methods, namely CBF and MVDR. CS has also been applied in an ocean setting for matched field localization [14, 15] and layer determination [16].

The data set is from the shallow water evaluation cell experiment 1996 (SWellEx-96) Event S5 [17, 18] which was collected on a 64-element vertical linear array. The array has uniform intersensor spacing 1.875 m and was deployed at waterdepth 16.5 m spanning 94.125–212.25 m. During the Event S5, from 23:15–00:30 on 10-11 May 1996 west of Point Loma, CA, two sources, a shallow and a deep, were towed simultaneously from 9 km southwest to 3 km northeast of the array at a speed of 5 knots (2.5 m/s). Each source was transmitting a unique set of tones.

Here, we are interested in the deep source towed at 54 m depth while at the vicinity of the closest point of approach

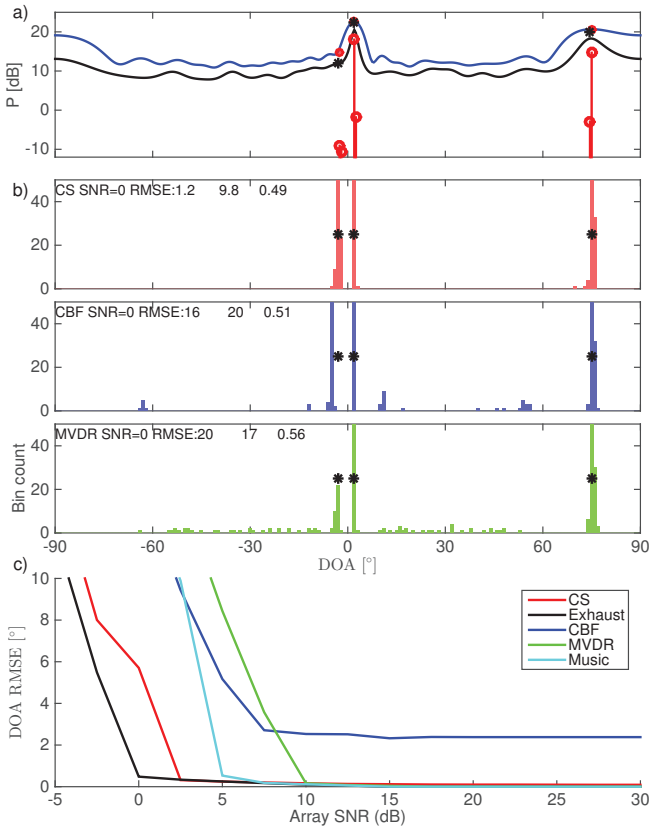

Fig. 1. (Color online) Multiple $L = 50$ snapshot example for 3 sources at DOAs $[-3,\ 2,\ 75]^\circ$ with magnitudes $[12,\ 22,\ 20]$ dB. At $\mathrm{SNR} = 0\,\mathrm{dB}$ a) spectra for CBF, MVDR, and CS (o) and unbiased CS (o, higher levels), and b) CS, CBF and MVDR histogram based on 100 Monte Carlo simulations, and c) CS, exhaustive-search, CBF, MVDR, and MUSIC performance versus SNR. The true source positions (*) are indicated in a) and b).

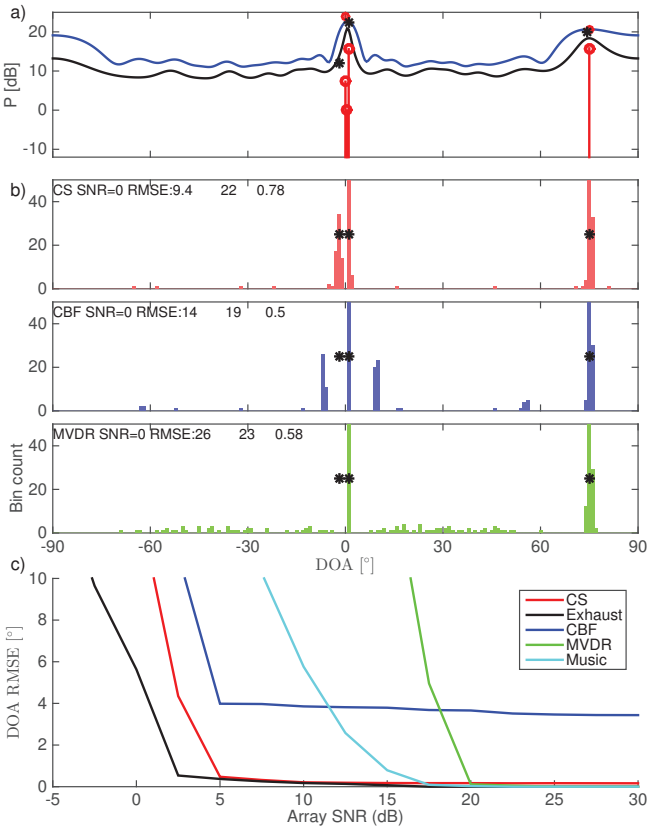

Fig. 2. (Color online) As Fig. 1 but with closer spaced sources $[-2,\ 1,\ 75]^\circ$.

(CPA) which was 900 m from the array and occurred around 00:15, 60 min into the event. The deep-towed source signal emitted a set of 9 frequencies [112, 130, 148, 166, 201, 235, 283, 338, 388] Hz at approximately 158 dB re 1μPa. The processed recording has duration of 1.5 min (covering 0.5 min before and 1 min after the CPA) sampled at 1500 Hz. It was split into 87 snapshots of 2^{12} samples (2.7 s) duration, i.e., with 63% overlap.

Figure 4 shows the multiple-snapshot CBF spatial spectrum, over the 50-400 Hz frequency range. Arrivals are detected not only at the transmitted tonal frequencies of the deep towed source but also at several other frequencies corresponding to the shallow-towed source tonal frequencies, weaker deep source frequencies, and the acoustic signature of the tow-ship.

Single-snapshot processing with CBF and CS at the deep source tonal set, contour plots in Fig. 5, indicates the presence of several multipath arrivals which are adequately stationary along the snapshots at the CPA. Due to the significant sound speed variation it is not straightforward to associate the reconstructed DOAs with specific reflections. The CBF map comprises 6 significant peaks but suffers from low resolution and artifacts due to sidelobes and noise. To choose the regularization parameter in the LASSO formulation for CS reconstruction, we solve iteratively Eq. (5) for a single snapshot with initial value $\mu = 2\|\mathbf{A}^H\mathbf{y}\|_\infty$, until the obtained estimate has a sparsity level of 10, as outlined in [8, 13]. The CS reconstruction results in improved resolution due to the sparsity constraint and significant reduction of artifacts in the map.

Combining the data from all the snapshots and processing with CBF, MVDR, and CS, reveals that MVDR fails to detect the coherent multipath arrivals; see line plots in Fig. 5. Again the peaks of CBF and CS are consistent but CS offers improved resolution.

We have here used higher sparsity for the single-snapshot processing to allow for identifying non-stationary paths. The non-stationary path can be seen in several of the contour plots, most prominently at 112, 130 and 201Hz. When perform-

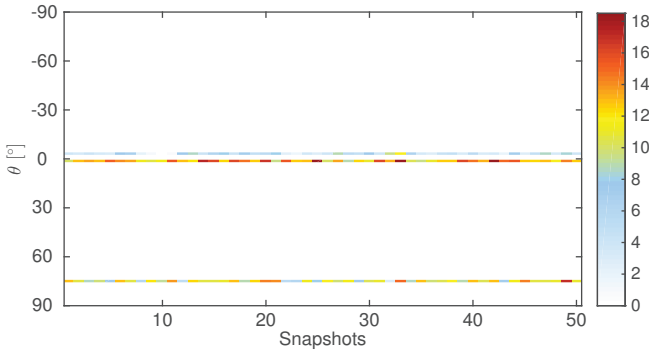

Fig. 3. (Color online) Power (linear) for the multiple snapshot case across azimuths and snapshots for one noise realization at $\mathrm{SNR} = 0\,\mathrm{dB}$ for the scenario with DOAs at $[-3,\ 2,\ 75]^\circ$.

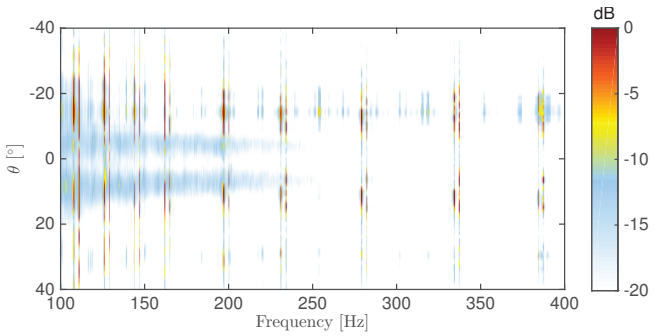

Fig. 4. Spatial CBF spectrum across frequency at the source's closest point of approach to the array.

ing multiple-snapshot processing where the solution is constrained to remain active at one azimuth (but with varying power), the stationary paths are most likely to contribute to the CS solution.

4. CONCLUSION

The estimation of multiple directions-of-arrival (DOA) is formulated as a sparse source reconstruction problem. This is efficiently solvable using compressive sensing (CS) as a least squares problem regularized with a sparsity promoting constraint. The resulting solution is the maximum a posteriori (MAP) estimate for both the single and multiple-snapshot formulations. The regularization parameter balances the data fit and the solution's sparsity. It is selected so that the solution is sufficiently sparse providing high-resolution DOA estimates. A procedure to find an adequate choice for the regularization parameter is described whereby the DOAs are obtained. For much more details on algorithm, implementation, and experimental validation see Refs. [8, 13].

CS provides high-resolution acoustic imaging both with single and multiple snapshot. The performance evaluation shows that for single snapshot data, CS gives higher resolution than CBF. For multiple snapshots, CS provides higher resolution than MVDR/MUSIC and the relative performance improves as the source DOAs move closer together.

5. REFERENCES

[1] D. Malioutov, M. Çetin, and A. S. Willsky. A sparse signal reconstruction perspective for source localization with sensor arrays. *IEEE Trans. Signal Process.*, **53**(8):3010–3022, 2005.

[2] A. Xenaki, P. Gerstoft, and K. Mosegaard. Compressive beamforming. *J. Acoust. Soc. Am.*, **136**(1):260–271, 2014.

[3] A. Xenaki and P. Gerstoft. Grid-free compressive beamforming. *J. Acoust. Soc. Am.*, **137**:1923–1935, 2015.

[4] H.L. Van Trees. *Optimum Array Processing (Detection, Estimation, and Modulation Theory, Part IV)*, chapter 1–10. Wiley-Interscience, New York, 2002.

[5] G. F. Edelmann and C. F. Gaumond. Beamforming using compressive sensing. *J. Acoust. Soc. Am.*, **130**(4):232–237, 2011.

[6] C. F. Mecklenbräuker, P. Gerstoft, A. Panahi, and M. Viberg. Sequential Bayesian sparse signal reconstruction using array data. *IEEE Trans. Signal Process.*, **61**(24):6344–6354, 2013.

[7] S. Fortunati, R. Grasso, F. Gini, M. S. Greco, and K. LePage. Single-snapshot DOA estimation by using compressed sensing. *EURASIP J. Adv. Signal Process.*, **120**(1):1–17, 2014.

[8] P. Gerstoft, A. Xenaki, and C. F Mecklenbräuker. Multiple and single snapshot compressive beamforming. *J Acoust. Soc. Am.*, 138(4):2003–2014, 2015.

[9] S. F. Cotter, B. D. Rao, K Engan, and K. Kreutz-Delgado. Sparse solutions to linear inverse problems with multiple measurement vectors. *IEEE Trans Signal Proc.*, 53:2477–2488, 2005.

[10] D. Wipf and B. Rao. An empirical bayesian strategy for solving the simultaneous sparse approximation problem. *IEEE Trans. Signal Process.*, **55**(7):3704–3716, 2007.

[11] E. Ollila. Multichannel sparse recovery of complex-valued signals using Huber's criterion. In *2015* 3rd *International Workshop on Compressed Sensing Theory and its Applications to Radar, Sonar, and Remote Sensing (CoSeRa),*, pages 1–4, Pisa, Italy, Jun. 17–19 2015.

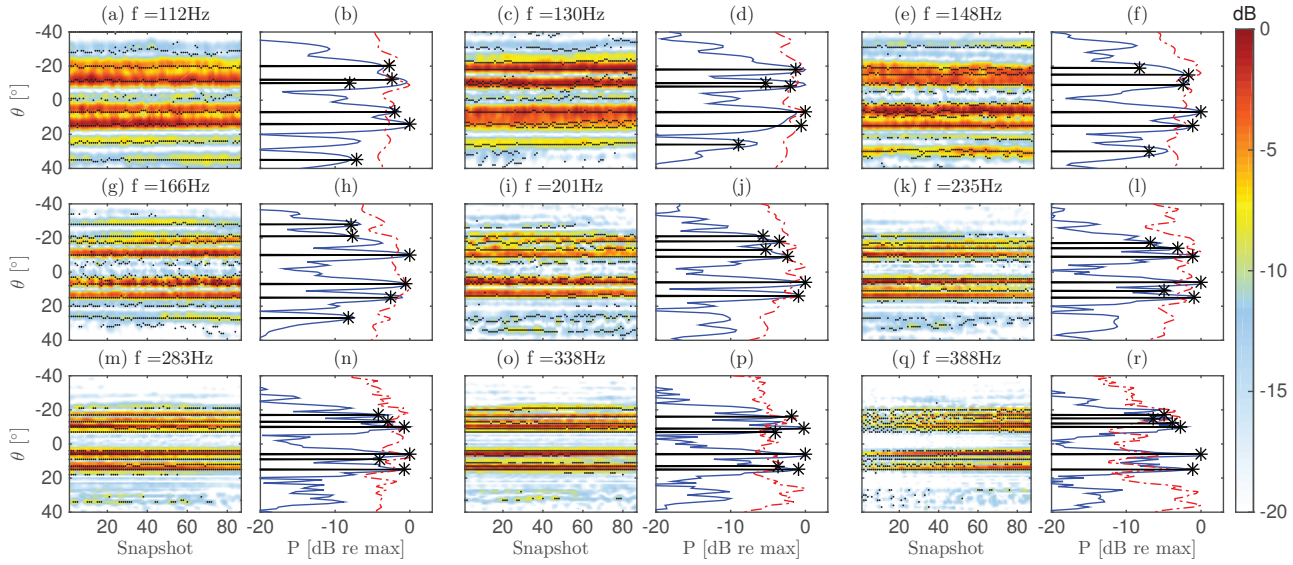

Fig. 5. Single (contour plots) and multiple (line plots) snapshot reconstruction at the transmitted frequencies with CS ($\star$), CBF (background color, solid) and MVDR (dashed). For the single snapshot we have assumed $K = 10$ sources while for the multiple snapshot $K = 6$.

[12] R. Tibshirani. Regression shrinkage and selection via the lasso. *J. Roy. Statist. Soc. Ser. B*, **58**(1):267–288, 1996.

[13] C. F. Mecklenbräuker, P. Gerstoft, and E. Zöchmann. Using the LASSO's dual for regularization in sparse signal reconstruction from array data. *Arxiv*, page 1502.04643, 2015.

[14] W. Mantzel, J. Romberg, and K. Sabra. Compressive matched-field processing. *J. Acoust. Soc. Am.*, **132**(1):90–102, 2012.

[15] P. A. Forero and P. A. Baxley. Shallow-water sparsity-cognizant source-location mapping. *J. Acoust. Soc. Am.*, **135**(6):3483–3501, 2014.

[16] C. Yardim, P. Gerstoft, W. S. Hodgkiss, and Traer J. Compressive geoacoustic inversion using ambient noise. *J. Acoust. Soc. Am.*, **135**(3):1245–1255, 2014.

[17] N. O. Booth, P. A. Baxley, J. A. Rice, P. W. Schey, W. S. Hodgkiss, G. L. D'Spain, and J. J. Murray. Source localization with broad-band matched-field processing in shallow water. *IEEE J Oceanic Eng.,*, **21**(4):400–411, 1996.

[18] G. L. D'Spain, J. J. Murray, W. S. Hodgkiss, N. O. Booth, and P. W. Schey. Mirages in shallow water matched field processing. *J Acoust. Soc. Am.*, **105**(6):3245, 1999.